



OPEN

SUBJECT AREAS:

VIRUS-HOST
INTERACTIONS

RETROVIRUS

VIRAL EVOLUTION

Characterization of red-capped mangabey tetherin: implication for the co-evolution of primates and their lentiviruses

Received
28 March 2014Accepted
11 June 2014Published
2 July 2014

Tomoko Kobayashi^{1*†}, Junko S. Takeuchi^{1*}, Fengrong Ren^{2*}, Kenta Matsuda^{3*}, Kei Sato^{1*}, Yuichi Kimura¹, Naoko Misawa¹, Rokusuke Yoshikawa¹, Yusuke Nakano^{1,4}, Eri Yamada¹, Hiroshi Tanaka², Vanessa M. Hirsch³ & Yoshio Koyanagi¹

¹Laboratory of Viral Pathogenesis, Institute for Virus Research, Kyoto University, Kyoto 6068507, Japan, ²Department of Bioinformatics, Medical Research Institute, Tokyo Medical and Dental University, Tokyo 1138510, Japan, ³Laboratory of Molecular Microbiology, National Institute of Allergy and Infectious Diseases, National Institutes of Health, Bethesda, Maryland 20892, USA, ⁴Department of Medical Virology, Faculty of Life Sciences, Kumamoto University, Kumamoto 8608556, Japan.

Correspondence and requests for materials should be addressed to K.S. (ksato@virus.kyoto-u.ac.jp)

* These authors contributed equally to this work.

† Current address: Laboratory of Animal Health, Department of Animal Science, Faculty of Agriculture, Tokyo University of Agriculture. 1737 Funako, Atsugi, Kanagawa 2430034, Japan.

Primate lentiviruses including human immunodeficiency virus type 1 (HIV-1) and simian immunodeficiency viruses (SIVs) evolved through the acquisition of antagonists against intrinsic host restriction factors, such as tetherin. It is widely accepted that HIV-1 has emerged by zoonotic transmission of SIV in chimpanzee (SIVcpz), and that SIVcpz Nef protein antagonizes chimpanzee tetherin. Although Nef of SIVcpz shares a common ancestor with that of SIVrcm, an SIV in red-capped mangabey (*Cercocebus torquatus*), it remains unclear whether SIVrcm Nef can antagonize tetherin of its natural host. In this study, we determine the sequence of red-capped mangabey tetherin for the first time and directly demonstrate that SIVrcm Nef is the *bona fide* antagonist of red-capped mangabey tetherin. These findings suggest that SIVrcm Nef is the functional ancestor of SIVcpz Nef. Moreover, molecular phylogenetic analyses reveal that tetherins of the genus *Cercocebus* have experienced adaptive evolution, which is presumably promoted by primate lentiviruses.

So far, more than 40 primate lentiviruses (PLVs) including human immunodeficiency viruses (HIVs) and simian immunodeficiency viruses (SIVs) have been identified¹. Understanding the evolutionary history of PLVs is one of the most important and interesting topics in the field of retrovirology. However, since PLVs have experienced multiple cross-species transmissions and complicated recombination, it is difficult to elucidate how genetic conflicts between the ancient PLVs and their respective host species resulted in evolution and diversification.

One way to approach this issue is to concentrate on the evolution and the diversity of specific accessory genes in PLVs. All PLVs identified so far encode 8 common genes: *gag*, *pol*, *env*, *tat*, *rev*, *vpr*, *vif*, and *nef*. In addition, the PLVs in the HIV-1 lineage encode an additional accessory gene, *vpu*, whereas those in the HIV-2 lineage encode the other unique gene, *vpx*². Interestingly, recent studies focusing on the interplay between viral and host proteins^{3–5} have provided lines of evidence for supporting “Red Queen hypothesis”⁶ or “evolutionary arms race”, which is an important assumption proposed for the co-evolution of PLVs and their host species. For instance, the accessory proteins such as Vif, Vpx, Vpu, and Nef encoded by PLVs have been acquired and evolved their abilities to antagonize cellular anti-PLV restriction factors such as apolipoprotein B mRNA editing enzyme, catalytic polypeptide-like 3G (APOBEC3G)⁷, SAM domain and HD domain 1 (SAMHD1)^{8,9}, and bone marrow stromal antigen 2 ([BST2], also known as tetherin, CD317, and HM1.24; hereinafter referred to as “tetherin”)^{10,11}. Tetherin impairs the release of nascent viral particles from virus-producing cells^{10,11}. In contrast to APOBEC3G and SAMHD1, which are antagonized by single accessory proteins Vif and Vpx respectively, PLVs acquired diverse strategies to antagonize tetherin^{5,12}. For instance, in Old World monkeys (OWMs; the family *Cercopithecidae*) and hominoids (the family *Hominidae*), most PLVs including SIVcpz from chimpanzee (*Pan troglodytes*; CPZ), SIVgor from gorilla (*Gorilla gorilla*; GOR), SIVsm from sooty mangabey (*Cercocebus atys*; SM), and SIVmac from rhesus macaque (*Macaca mulatta*; RM) antagonize tetherins of their own hosts by their



Nef proteins^{13–16}. On the other hand, *vpu* is encoded only in seven out of the more than 40 PLVs identified: SIVgsn from greater-spot nosed monkey (*Cercopithecus nictitans*), SIVmon from mona monkey (*Cercopithecus mona*), SIVmus from moustached monkey (*Cercopithecus cephus*), SIVden from Dent's mona monkey (*Cercopithecus denti*), SIVcpz, SIVgor, and HIV-1 from human (*Homo sapiens*; HU)⁵. Of note, certain *vpu*-encoding SIVs from OWMs (SIVgsn, SIVmon, SIVmus, and SIVden) and HIV-1 antagonize tetherins of their own hosts by their Vpu proteins^{10,11,14,17–19}. These findings strongly suggest that PLVs have adapted to their hosts by acquiring the anti-tetherin factors at each adaptation process, and therefore, that the relationship between tetherin and viral antagonists can be a clue to reveal the evolutionary diversification of PLVs.

It is widely accepted that two HIVs, HIV-1 and HIV-2, have respectively emerged from independent zoonotic transmission of SIVs to HU around 100 years ago^{20–22}. HIV-1 has risen out of SIVcpz from CPZ to HU^{23,24}, while HIV-2 has resulted from zoonotic infection of SIVsm from SM²⁵. Also, it has been estimated that SIVcpz has emerged by the recombination of two lineages of SIVs: SIVgsn/mon/mus and SIVrcm from red-capped mangabey (*Cercocebus torquatus*; RCM)²⁶. Since SIVcpz Nef is phylogenetically similar to SIVrcm Nef, it seems conceivable that the ancestor of SIVcpz Nef is SIVrcm Nef^{5,14}. Moreover, because SIVcpz Nef is able to counteract CPZ tetherin¹⁴, it has been hypothesized that SIVrcm Nef is the antagonist of RCM tetherin^{5,27}. However, the sequence of RCM tetherin has not yet determined, and it remains unknown whether SIVrcm Nef is the *bona fide* antagonist of RCM tetherin. In this study, we determine the sequence of RCM tetherin for the first time and directly demonstrate that SIVrcm Nef counteracts antiviral activity of RCM tetherin. Moreover, phylogenetic analyses of 47 primate tetherin sequences reveal that tetherins of the genus *Cercocebus* including RCM and SM are under positive selection.

Results

Phylogeny reconstruction of 47 primate tetherins. In order to directly elucidate the interplay between SIVrcm Nef and RCM tetherin, we set out to determine the sequence of RCM tetherin. The sequencing analyses of genomic DNA isolated from six wild-caught RCMs^{28,29} revealed that five out of the six open reading frames (ORFs) of RCM tetherin were identical, while a RCM tetherin displayed a double peak at nucleotide position 60 (GAC or GAT; synonymous mutation). These results imply the presence of polymorphism in RCM tetherin.

As shown in Figure 1a, compared with the amino acid sequence of RCM tetherin, HU tetherin displayed the 5-amino acid deletion (¹⁴GDIWK¹⁸) in the cytoplasmic domain, and HU and CPZ tetherins showed the 2-amino acid insertion (³⁰GI³¹) in the transmembrane domain, both of which are in line with the previous observations^{13,14,17,18,27,30}. The phylogenetic tree of 47 primate tetherins reconstructed by using maximum likelihood (ML) method (Figure 1b) revealed that the two RCM tetherins, which are newly sequenced in this study, are clustered with SM tetherins with stronger bootstrap support (87%), suggesting that RCM tetherin is most closely related to SM tetherin. Because only RCM and SM are the monkeys belonging to the genus *Cercocebus* among the 27 OWMs (the family *Cercopithecidae*; Table 1), this result is reasonable.

Positive selection detected in the evolution of primate tetherin. The nonsynonymous to synonymous rate ratios (dN/dS) inferred by using a free-ratio model in the PAML package are shown on the ML tree (Figure 1b), which varied among the branches. Since a dN/dS value significantly greater than one is an indicator of positive selection, our result indicates that positive selection probably operated on the tetherin gene episodically during primate evolution. This result is consistent with that obtained in previous studies^{31,32}.

The two pairs of site models in PAML produced similar results and the result obtained from M7 (neutral model) versus M8 (selection model) comparison is shown in Figure 1c. The dN/dS ratio was significantly greater than one for full-length tetherin, cytoplasmic tail, and transmembrane domains. These findings indicate that the functionally important regions of tetherin have evolved under strong positive selection, which agreed with previous reports^{31–33}. The site model analysis also identified three codons, 9, 14, and 17, to be under positive selection with posterior probability greater than 0.95 (Figure 1d). Two of them, codons 9 and 14, were also detected by the random effects likelihood (REL) analysis implemented in the HyPhy package with Bayes factor greater than 50 (Figure 1e; these sites are also indicated with green asterisks in Figure 1a). Although these two sites have been reported by a previous study in which 20 primate tetherins were analyzed³¹, our results further suggest that they may have experienced positive selection in the evolution of many primate lineages, because more primate tetherins were included in our analysis. Moreover, the codon 41, which has been reported to be a positively selected site in a previous study³¹, was detected in our analysis as well with posterior probability of 0.841 (Figure 1d).

Furthermore, the branch-site tests in PAML revealed that the likelihood ratio test was significant with $P < 0.01$ in the analysis of the *Cercocebus* clade, suggesting that positive selection has most likely operated on *Cercocebus* tetherins (Figure 1f). On the other hand, no significant positive selection was detected for RCM clade, probably because only two highly similar sequences were included in this clade. In addition, the branch-site analysis identified six codons, 10, 14, 39, 93, 103, and 187, to be positively selected sites in the *Cercocebus* clade (Figure 1f; these sites are also indicated with pink asterisks in Figure 1a), and three out of the six sites, 93, 103, and 187, are located in the extracellular domain. In this regard, it has been recently reported that human tetherin directly binds to immunoglobulin-like transcript 7 (ILT7), a cellular molecule specifically expressed on plasmacytoid dendritic cells, through its extracellular domain and modulates ILT7-mediated signaling leading to the production of type I interferons and proinflammatory cytokines³⁴. Therefore, it is possible that these three sites may associate with the interaction of tetherin and ILT7 in the genus *Cercocebus*. Taken together, here we firstly demonstrated that *Cercocebus* tetherins have evolved under stronger positive selection and also identified six codons which may be functionally important.

Antagonism of RCM tetherin by SIVrcm Nef. We then assessed the interplay of RCM tetherin and SIVrcm Nef. Western blotting (Figure 2a) and TZM-bl assay (Figure 2b) revealed that increasing concentrations of CPZ, SM and RCM tetherins resulted in a dose-dependent decrease in the release of nascent viral particles. We then investigated whether SIVrcm Nef has the ability to antagonize RCM tetherin. As shown in Figure 2a, the Nefs of SIVcpz, SIVsm, and SIVrcm did not affect the expression levels of tetherins and Gag (Figure 2a), which is consistent with previous reports^{16,35}. Moreover, we revealed that the Nefs of 3 SIVrcm isolates, strains GAB1, NG411, and 02CM8081, enhanced virus release in the presence of RCM tetherin (Figures 2a and 2b). These findings directly demonstrate that SIVrcm Nef is the *bona fide* antagonist of RCM tetherin, and further support the hypothesis that the anti-tetherin ability of SIVcpz Nef is originated from that of SIVrcm Nef.

In the cytoplasmic tail of *Cercocebus* tetherins, we found a novel positively selected site positioned at 10 (Arginine in RCM and SM tetherins; Figure 1a) with posterior probability greater than 0.95 (Figure 1f). In this regard, previous papers have reported that human tetherin but not OWM tetherins (e.g., RM and AGM tetherins) has the ability to induce NFκB-dependent proinflammatory signaling, and that certain amino acids in the cytoplasmic tail of human tetherin (Figure 1a, with shading in pale blue) are associated with

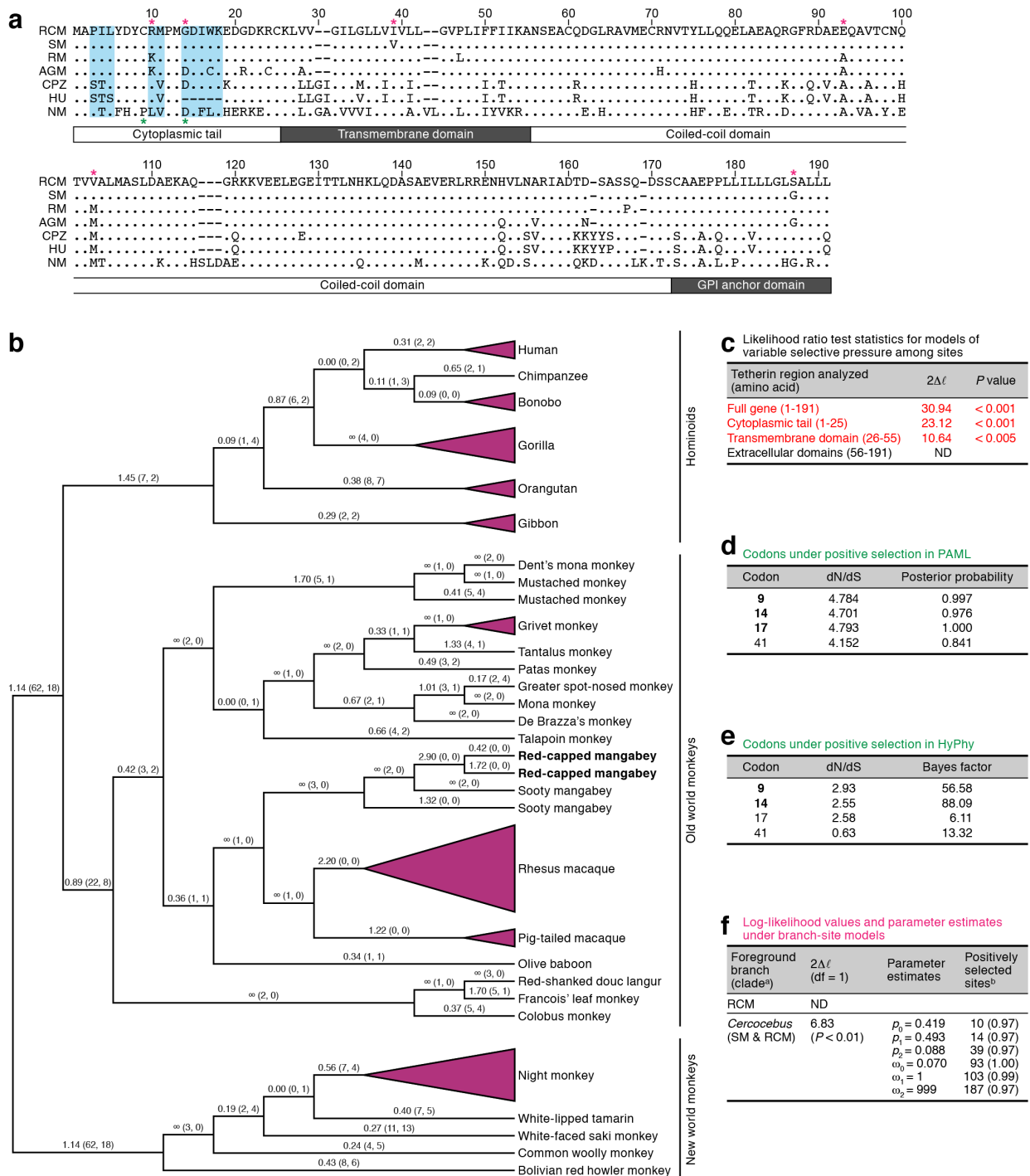


Figure 1 | Positive selection detected in primate tetherin. (a) Amino acid sequences of primate tetherin. RCM tetherin (GenBank accession number AB907706; determined in this study), SM tetherin (FJ864713), RM tetherin (FJ943432), African green monkey (*Chlorocebus aethiops*; AGM) tetherin (FJ943430), CPZ tetherin (NM_001190480), HU tetherin (NM_004335), and night monkey (*Aotus vociferans*; NM) tetherin (FJ638415) are respectively shown. The numbers indicate the amino acid positions in NM tetherin. The two positively selected sites (positioned at 9 and 14), which are determined by both site model of PAML (Figure 1d) and REL method of HyPhy (Figure 1e), are indicated with green asterisks. The six amino acids (positioned at 10, 14, 39, 93, 103, and 187) inferred to be under positive selection in *Cercocebus* tetherin (the clade of RCM and SM tetherins) (Figure 1f) are indicated with pink asterisks. The amino acids, which are putatively associated with the ability to induce NFκB-dependent signaling³⁶, are indicated with shading in pale blue. (b) Phylogenetic tree of 47 primate tetherins reconstructed using ML method. The tree was rerooted with the NWM clade. The dN/dS ratios are shown on each branch and the numbers in parenthesis represent nonsynonymous (left) and synonymous (right) changes, respectively. (c) The positive selection detected in different regions of the tetherin gene. The regions inferred to be under positive selection with statistical significance are represented in red. ND, not detected ($2\Delta\ell = -0.000002$). (d and e) Positively selected sites identified in our analyses. In panel d, the codons under positive selection identified by PAML with posterior probability > 0.95 are shown in bold. In panel e, the codons under positive selection inferred by HyPhy with Bayes factor > 50 are shown in bold. (f) The result obtained from the two-branch-site analyses for RCM and *Cercocebus* clades. All PAML analyses were performed under two models of codon usage, F61 and F3x4, and they yield consistent results. ^a, All nodes/branches within RCM and the *Cercocebus* clades were respectively designated as the foreground branches. ^b, The number in parenthesis represents posterior probability.



Table 1 | GenBank accession numbers of primate tetherins used in this study

Family/infracorder ^a	Common name ^b	Scientific name	Accession number ^c	
<i>Hominidae</i> (Hominoids)	Human	<i>Homo sapiens</i>	AK223124	
	Human	<i>Homo sapiens</i>	NM_004335	
	Chimpanzee	<i>Pan troglodytes</i>	NM_001190480	
	Bonobo	<i>Pan paniscus</i>	HM136907	
	Bonobo	<i>Pan paniscus</i>	XM_003817802	
	Gorilla	<i>Gorilla gorilla</i>	GQ925926	
	Gorilla	<i>Gorilla gorilla</i>	HM136906	
	Gorilla	<i>Gorilla gorilla</i>	XM_004060266	
	Orangutan	<i>Pongo pygmaeus</i>	HM136908	
	Orangutan	<i>Pongo abelii</i>	NM_001172587	
	Gibbon	<i>Hylobates agilis</i>	HM136910	
	Gibbon	<i>Nomascus leucogenys</i>	HM136909	
	<i>Cercopithecoidea</i> (OWMs)	Dent's mona monkey	<i>Cercopithecus denti</i>	HE680870
		Mustached monkey	<i>Cercopithecus cephus</i>	GQ864267
Mustached monkey		<i>Cercopithecus cephus</i>	GQ925925	
Grivet monkey		<i>Chlorocebus aethiops</i>	FJ943430	
Grivet monkey		<i>Chlorocebus aethiops</i>	HM136912	
Tantalus monkey		<i>Chlorocebus tantalus</i>	FJ345303	
Patas monkey		<i>Erythrocebus patas</i>	HM136911	
Greater spot-nosed monkey		<i>Cercopithecus nictitans</i>	GQ925923	
Mona monkey		<i>Cercopithecus mona</i>	GQ925924	
De Brazza's monkey		<i>Cercopithecus neglectus</i>	HE680871	
Talapoin monkey		<i>Miopithecus talapoin</i>	HM136913	
Red-capped mangabey		<i>Cercocebus torquatus</i>	This study^d	
Red-capped mangabey		<i>Cercocebus torquatus</i>	This study^e	
Sooty mangabey		<i>Cercocebus atys</i>	FJ864713	
Sooty mangabey		<i>Cercocebus atys</i>	FJ864714	
Rhesus macaque		<i>Macaca mulatta</i>	FJ943431	
Rhesus macaque		<i>Macaca mulatta</i>	FJ943432	
Rhesus macaque		<i>Macaca mulatta</i>	GQ304749	
Rhesus macaque		<i>Macaca mulatta</i>	HM136914	
Rhesus macaque		<i>Macaca mulatta</i>	HM775182	
Rhesus macaque		<i>Macaca mulatta</i>	NM_001161666	
Pig-tailed macaque		<i>Macaca nemestrina</i>	FJ914988	
Pig-tailed macaque		<i>Macaca nemestrina</i>	FJ914989	
Olive Baboon		<i>Papio anubis</i>	XM_003915138	
Red-shanked douc langur		<i>Pygathrix nemaeus</i>	HM136916	
Francois' leaf monkey		<i>Trachypithecus francoisi</i>	HM136917	
Colobus monkey		<i>Colobus guereza</i>	HM136915	
<i>Platyrrhini</i> (NWMs)		Night monkey	<i>Aotus lemurinus</i>	FJ638414
	Night monkey	<i>Aotus vociferans</i>	FJ638417	
	Night monkey	<i>Aotus vociferans</i>	FJ638418	
	Night monkey	<i>Aotus vociferans</i>	FJ638415	
	White-lipped tamarin	<i>Saguinus labiatus</i>	HM136918	
	White-faced saki monkey	<i>Pithecia pithecia</i>	HM136920	
	Common woolly monkey	<i>Lagothrix lagothricha</i>	HM136922	
	Bolivian red howler monkey	<i>Alouatta sara</i>	HM136921	

^aFamily (*Hominidae* and *Cercopithecoidea*) and infraorder (*Platyrrhini*) are presented in italic. Popular name of each family/infracorder is presented in parenthesis. OWMs, old world monkeys; NWMs, new world monkeys.

^bThe common name of each primate is identical to that in Figure 1B.

^cThe GenBank accession numbers (<http://www.ncbi.nlm.nih.gov/genbank/>) of tetherins are listed.

^dAB907706.

^eAB907707.

this activity^{36–38}. It is particularly noteworthy that the site 10 detected to be under positive selection in *Cercocebus* tetherin is located in this region and has the same amino acid (arginine) with that in human tetherin (Figure 1a). This raises a hypothesis that *Cercocebus* tetherin has evolutionarily acquired this NFκB-mediated signaling capacity. To address this possibility, tetherin expression plasmids were cotransfected with an NFκB-luciferase reporter plasmid³⁹ and a *vpu*-deficient HIV-1-producing plasmid⁴⁰ into 293T cells. However, although we detected the induction of NFκB-mediated activation by human tetherin, *Cercocebus* tetherins including RCM and SM tetherins did not elicit this activity (Figure 3b). Although a previous study has shown that CPZ tetherin partially induces this NFκB-mediated signaling³⁶, this effect was not observed in our assay

(Figure 3b). This may be due to the addition of KGC tag at the N-terminus of tetherin in our study. These results suggest that an arginine residue at the site 10 is not associated with the gain-of-function to induce NFκB-mediated signaling.

Gain-of-function evolution of SIVcpz Nef. As described above, phylogenetic analyses has assumed that SIVcpz is the recombinant of two OWM SIV lineages, SIVgsn/mon/mus and SIVrcm²⁶. Consistent with previous reports^{5,14}, we confirmed that SIVcpz Nef is phylogenetically closer to SIVrcm Nef than SIVgsn, SIVmon, and SIVmus Nefs (Figure 4a). We then directly evaluated the functional evolution process of SIV Nefs in terms of anti-tetherin ability. Although SIVcpz Nef efficiently antagonized CPZ tetherin, the

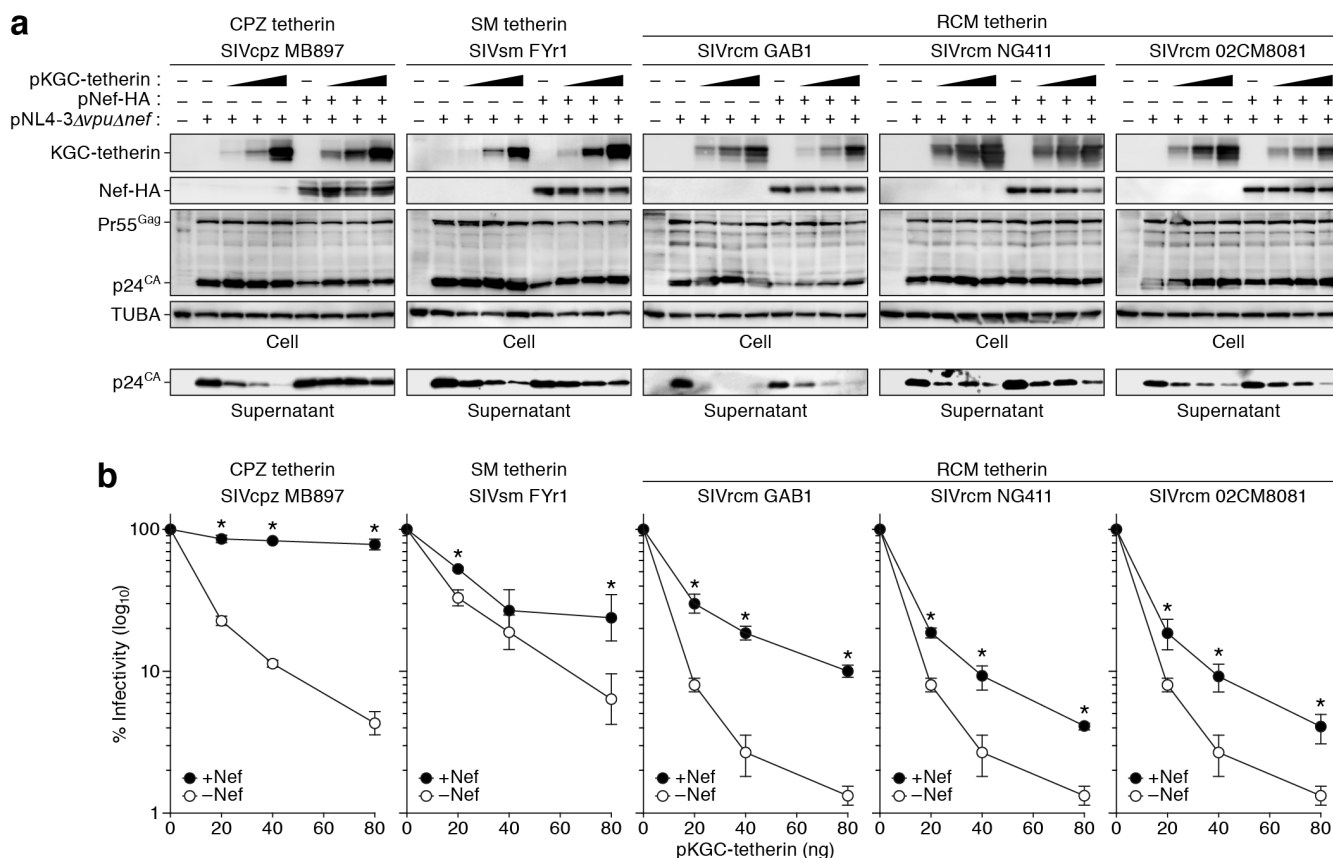


Figure 2 | Anti-viral activity of RCM tetherin and antagonistic ability of SIVrcm Nefs. (a) Western blotting. Representative results are shown. Blots have been cropped; full uncropped blots are available as Supplementary Figure 1. (b) TZM-bl assay. The data represents the percentage of infectivity compared to the values without tetherin \pm SD. The assay was performed in triplicate. The statistical difference ($*P < 0.05$) is determined by Student's *t* test.

counteraction efficacy of OWM SIV Nefs including SIVsm, SIVrcm and SIVgsn/mon/mus was significantly lower than that of SIVcpz Nef (Figures 4b and 4c). These results suggest that the difference in anti-tetherin activity (Figure 2) is not related to Nef but is due to the differences between RCM and CPZ tetherins. On the other hand, it was of interest that SIVcpz Nef counteracted RCM tetherin in comparable to SIVrcm Nefs (Figures 4d and 4e). Because SIVcpz Nef is able to antagonize RCM tetherin in addition to CPZ tetherin, these findings suggest that SIVcpz Nef has accomplished a gain-of-function during evolution.

Discussion

In this study, we have determined the sequence of RCM *tetherin*. In addition, we have demonstrated that RCM tetherin has the ability to

impair the release of nascent viral particles and that SIVrcm Nef is the *bona fide* antagonist against RCM tetherin. Although the two concepts: (i) SIVrcm Nef counteracts RCM tetherin; and (ii) this ability is succeeded to SIVcpz Nef, have been proposed elsewhere^{5,27}, no direct evidence has been shown so far. Therefore, to our knowledge, this is the first report directly elucidating the interplay between SIVrcm Nef and RCM tetherin (Figure 2). Moreover, we here firstly performed the phylogenetic analysis of primate tetherins with *Cercocebus* tetherins including SM and RCM tetherins and revealed that stronger positive selection occurred in the evolution of *Cercocebus* tetherins (Figure 1).

To better understand the Red Queen dynamics in the co-evolution of PLVs and primates, our findings should be compared with the evolutionary interplay between Vpx and simian SAMHD1. To antagonize the anti-viral ability of simian SAMHD1, certain SIVs including SIVrcm degrade SAMHD1 by a viral protein, Vpx. In this regard, Etienne et al. have recently demonstrated that *vpx*, which is located at the recombination site of SIVrcm and SIVgsn/mon/mus, was lost during the emergence of SIVcpz and that SIVcpz does not possess any anti-CPZ SAMHD1 factor(s)⁴¹. When compared to the evolutionary interplay between SIV Vpx and SAMHD1, our findings on the relationship between SIV Nef and tetherin suggest that anti-tetherin ability was more crucial for PLVs, at least for SIVcpz, to adapt and expand in the new host because SIVcpz Nef has successfully inherited its anti-tetherin ability from SIVrcm Nef. Moreover, SIVcpz Nef has acquired the ability to antagonize CPZ tetherin without the loss of anti-RCM tetherin activity, indicating that SIVcpz Nef has made the way through a gain-of-function evolution (Figure 4). To our knowledge, here we demonstrated that SIVcpz Nef is able to antagonize OWM tetherin for the first time. Our findings can be a milestone to decipher the complicated co-evolutionary process between PLVs and primates.

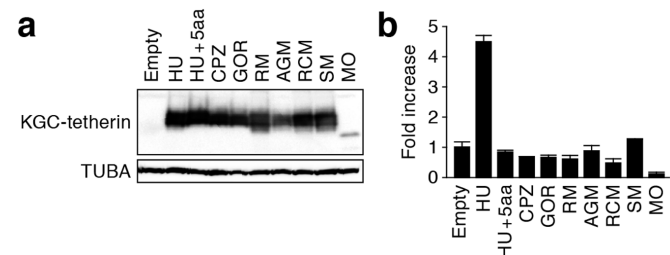


Figure 3 | Ability of primate tetherins to induce NF κ B-dependent signaling. (a) Western blotting. Representative results are shown. Blots have been cropped; full uncropped blots are available as Supplementary Figure 2. (b) Luciferase assay. The data represents the average of fold induction of luciferase activity compared to the empty vector-transfected cells with SD. The assay was performed in triplicate.

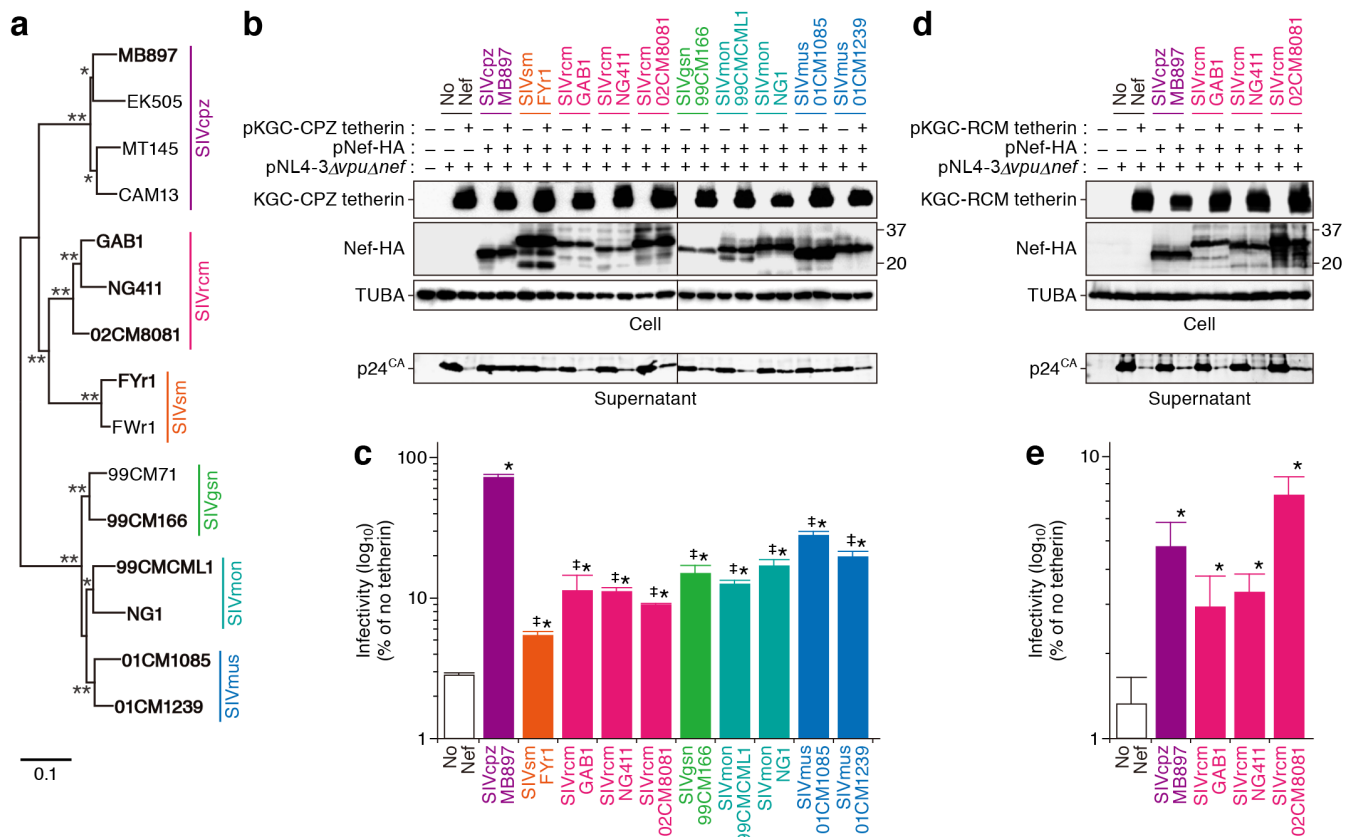


Figure 4 | Gain-of-function evolution of SIVcpz Nef. (a) Phylogenetic tree of SIV Nef. The strains indicated in bold were used in the experiments shown in panels (b–e). Bootstrap values are shown as follows: *, >50%; **, >80%. (b–e) Anti-viral effect of CPZ and RCM tetherins and the antagonism by SIV Nefs. (b and d) Western blotting. Representative results are shown. The number on the right of blots indicates kilodalton. Blots have been cropped; full uncropped blots are available as Supplementary Figure 3. (c and e) TZM-bl assay. The data represents the percentage of infectivity compared to the values without tetherin with SD. The assay was performed in triplicate. The statistic difference is determined by Student's *t* test. *, $P < 0.05$ versus no Nef; ‡, $P < 0.05$ versus SIVcpz Nef.

As described in the beginning of this paper, HIV-2 has resulted from the zoonotic infection of SIVsm from SM²⁵, while SIVrcm in RCM is one of the ancestral viruses of SIVcpz giving rise to HIV-1²⁶. These insights imply that the ancestors of these two HIVs have passed through the genus *Cercocebus*, namely SM or RCM. In this study, we firstly performed molecular phylogenetic analyses of primate tetherins with the genus *Cercocebus* and revealed that positive selection had operated on *Cercocebus* tetherins (Figure 1). Since it has been estimated that the genus *Cercocebus* has evolutionary diversified around 4–4.85 million years ago^{42,43}, the observed positive selection probably occurred after the divergence of the genus *Cercocebus*. In fact, a recent paper has suggested that PLVs had already existed at least 12 million years ago⁴⁴. Therefore, it is plausible that a Nef-like protein encoded by ancient PLV(s) can be regarded as a selective pressure against *Cercocebus* tetherins. Moreover, it is of interest that the 2 types of genetic deletion in *CCR5*, *CCR5Δ24*⁴⁵ and *CCR5Δ26*⁴⁶, have been observed in the population of genus *Cercocebus* including RCM and SM, and that the homozygous mutants are resistant to *CCR5*-tropic SIV infections. To circumvent the restriction at the entry step of infection, some SIVrcm and SIVsm have acquired the ability to use alternative coreceptors for their infections presumably as a result of genetic conflict between viruses and hosts^{45,46}. Although SIVsm is nonpathogenic in SM, it is conceivable that the ancestors of the genus *Cercocebus* have been subjected to stronger selective pressure from pathogenic PLVs and that the genetic conflict between pathogenic PLVs and the genus *Cercocebus*, including ancient Nef and *Cercocebus* tetherins, might have occurred in their evolutionary history.

Methods

Sequencing PCR. Blood was collected from six wild-caught RCMs in Nigeria according to the Guide for the Care and Use of Laboratory Animals⁴⁷ under a NIAID Animal Care and Use Committee-approved protocol^{28,29}. RCM genomic DNA was isolated from cryopreserved peripheral blood mononuclear cells^{28,29}, and PCR was performed by using *PfuUltra* High Fidelity DNA polymerase (Agilent Technologies) and the following primers: 5'-CAG CTA GAG GGG AGA TCT GGA TG-3'; 5'-CTC ACT GAC CAG CTT CCT GGG-3', which were used in a previous study³¹. The obtained PCR products (approximately 2 kb) were purified by gel extraction and directly sequenced by using BigDye Terminator v3.1 cycle sequencing kit (Applied Biosystems) with the two primers described above and the following 4 primers: 5'-GGA CTT CAC CAG ACC CTG AA-3'; 5'-TTC AGG GTC TGG TGA AGT CC-3'; 5'-TCT CTC CTT TGC TCC CAA AA-3'; 5'-TTT TGG GAG CAA AGG AGA GA-3'. The sequencing PCR was performed by using ABI Prism 3130 xl genetic analyzer (Applied Biosystems), and the data was analyzed by Sequencher v5.1 software (Gene Codes Corporation).

Phylogenetic analyses. The two RCM tetherins newly sequenced in this study (note that five out of the six analyzed RCM tetherin sequences were identical) was aligned with 45 primate tetherins (listed in Table 1) by using ClustalW implemented in MEGA5⁴⁸. The resulting alignment was verified manually at amino acid level. Then the phylogenetic tree of 47 primate tetherins was reconstructed using both neighbour-joining (NJ) method⁴⁹ with MEGA5 and ML method with PhyML⁵⁰. Since the two methods yield almost identical topology, the unrooted ML tree was used for further analyses.

The detection of positive selection was conducted as follows: first, to detect the positive selection across various primate lineages, two pairs of site models implemented in the PAML package v 4.7⁵¹ were used to conduct the likelihood ratio tests: M1 (neutral model) versus M2 (selection model) and M7 (neutral model) versus M8 (selection model). The REL model in HyPhy was also employed to this analysis. Second, to calculate the dN/dS ratio of each primate tetherin, a free-ratio branch model in PAML was performed, which assumes an independent dN/dS ratio for each branch of the tree. Third, since we were particularly interested in whether the RCM and *Cercocebus* clades have evolved under positive selection, the branch-site model in



PAML was further applied to our analyses. This model allows dN/dS ratio vary both among sites and branches, which is useful for detecting positive selection along a particular lineage or clade (pre-specified as foreground branches) with positively selected site identified^{32,52–55}. We conducted two branch-site tests in which RCM and the *Cercopithecus* clades were designated as the foreground branches, respectively.

SIV Nef sequences were aligned by using ClustalW implemented in MEGA5⁴⁸. The phylogenetic tree of SIV Nef was reconstructed using NJ method⁴⁹ with MEGA5.

Plasmid construction. To construct tetherin expression plasmids tagged with Kusabira green C (KGC) at N-termini, tetherin ORFs were inserted into the *KpnI-XhoI* site of phmKGC-MC vector (Medical and Biological Laboratories, Inc.). The ORFs of HU tetherin (GenBank accession number NM_004335), AGM tetherin (FJ943430), and mouse (*Mus Musculus*; MO) tetherin (NM_198095) were used in our previous report¹⁸. CPZ tetherin (XM_512491), GOR tetherin (GQ925926), RM tetherin (FJ943432), and SM tetherin (FJ864713), and RCM tetherin (AB907706, determined in this study) were generated by overlap extension PCR using artificially synthesized oligonucleotides (Greiner bio-one). The ORF of the 5 amino acid (¹⁴GDIWK¹⁸)-inserted HU tetherin (designated “HU + 5aa”) was prepared by overlap extension PCR using HU tetherin expression plasmid as the template and the following primers: 5'-GGG GTA CCC CCA TGG CAT CTA CTT CGT ATG-3'; 5'-TTT CTT CCA AAT GTC ATC CAT GGG CAC TCT GCA ATA-3'; 5'-GAT GAC ATT TGG AAG AAA GAC GGG GAT AAG CGC TGT-3'; 5'-CCG CTC GAG CGG ATC TCA CTG CAG CAG AGC GCT GA-3'. To construct SIV Nef expression plasmids tagged with Hemagglutinin (HA) at the C-termini, HA was added at the C-termini of Nef ORFs by PCR and the Nef-HA fragments were then inserted into the *XbaI-MluI* site of pCGCG-IRES-EGFP vector (kindly provided by Dr. Frank Kirchhoff⁵⁶). The ORFs of SIVsm Nef (strain FyR1 [DQ092760]), 2 SIVrcm Nefs (strains NG411 [AF349680] and 02CM8081 [HM803689]), SIVgsn Nef (strain 99CM166 [AF468659]), 2 SIVmon Nefs (strains 99CMCLM1 [AY340701] and NG1 [GQ925927]), and 2 SIVmus Nefs (strains 01CM1085 [AY340700] and 01CM1239 [EF070330]) were obtained from GeneArt Gene Synthesis service (Life Technologies). The ORF of SIVrcm Nef (strain GAB1 [AF382829]) was generated by overlap extension PCR using artificially synthesized oligonucleotides (Greiner bio-one). The ORF of SIVcpz Nef (strain MB897 [EF535994]) was prepared by overlap extension PCR using pMB897 (an infectious molecular clone of SIVcpz strain MB897 [JN835461]; kindly provided by Dr. Beatrice Hahn⁵⁷) as the template and the following primers: 5'-TTA ATA CCT AGT CTA GAC TAG ATG GGA AAC AAA TGG TCA AAA AGT AGC-3'; 5'-TAG CGA CGC GTC GGC GAG ATC TCT AAG CGT AAT CTG GTA CGT CGT ATG GGT AGA TAT CGC AGT CTT TGT AGT ACT CCG GAT GC-3'. To construct pNL4-3Δ*vpu*Δ*nef* (an HIV-1-producing plasmid with defects in *vpu* and *nef*), pNL43-Udel (a *vpu*-deficient HIV-1-producing plasmid, based on HIV-1 strain NL4-3 [M19921]; kindly provided by Dr. Klaus Strebel⁴⁰) was digested with *XhoI*, blunt-ended, and then self-ligated. The sequencing PCR was performed by using ABI Prism 3130 *xl* genetic analyzer (Applied Biosystems), and the data were analyzed by Sequencher v5.1 software (Hitachi).

Cell culture and transfection. 293T cells and TZM-bl cells (obtained through NIH AIDS Research and Reference Reagent Program) were maintained in Dulbecco's modified Eagle medium (Sigma) containing FCS and antibiotics. Transfection was performed by using Lipofectamine 2000 (Life Technologies) according to the manufacturer's protocol. Various amounts of KGC-tagged tetherin expression plasmids (0, 20, 40, 80 ng) and pNL4-3Δ*vpu*Δ*nef* (1,500 ng) were cotransfected with or without the expression plasmids of SIV Nefs of their natural hosts (400 ng) into 293T cells. At 48 hours post-transfection, the culture supernatants and transfected cells were harvested and were respectively used for TZM-bl assay and Western blotting as described below.

Viral budding and Western blotting. The culture supernatant harvested at 48 hours post-transfection was centrifuged and then filtered through a 0.45-μm-pore-size filter (Milipore) to produce virus solution. The infectivity of virus solution was measured by TZM-bl assay as previously described^{18,19,58}. Briefly, 10 μl of the virus solution was inoculated into TZM-bl cells in 96-well plate (Nunc), and the β-galactosidase activity was measured by using the Galacto-Star mammalian reporter gene assay system (Roche) and a 2030 ALBO X multilabel counter instrument (PerkinElmer) according to the manufacturers' procedure. Western blotting was performed as previously described^{18,19,58} by using the following antibodies: anti-p24 polyclonal antibody (ViroStat), anti-KGC antibody (clone 21B10; Medical and Biological Laboratories, Inc.), anti-HA antibody (3F10; Roche), and anti-α-Tubulin (TUBA) antibody (DM1A; Sigma). For the virus solution, 500 μl of the virus solution was ultracentrifuged at 100,000 × *g* for 1 hour at 4°C using a TL-100 instrument (Beckman). The pellet was lysed with 1 × SDS buffer, and the lysate was used for SDS-PAGE/Western blotting. For the transfected cells, the cells were lysed with 1 × SDS buffer, and the lysate was used for SDS-PAGE/Western blotting.

NFκB reporter assay. One hundred nanogram of either respective tetherin expression plasmid or parental empty vector (phmKGC-MC) was cotransfected with 25 ng of an NFκB-luciferase reporter plasmid (p55A2-Luc; kindly provided by Dr. Takashi Fujita³⁹), 250 ng of a *vpu*-deficient HIV-1-producing plasmid (pNL43-Udel; kindly provided by Dr. Klaus Strebel⁴⁰), and 125 ng of pUC19 plasmid into 293T cells. At 48 hours post-transfection, the cells were harvested and used for Western blotting and luciferase assay. Luciferase assay was performed as previously described⁵⁸.

Statistical analyses. The data expressed as average with standard deviation (SD), and significant differences ($P < 0.05$) were determined by Student's *t* test.

- Klatt, N. R., Silvestri, G. & Hirsch, V. Nonpathogenic simian immunodeficiency virus infections. *Cold Spring Harb. Perspect. Med.* **2**, a007153 (2012).
- Desrosiers, R. C. Nonhuman Lentiviruses. *Fields Virology* (eds Knipe, D. M. & Howley, P. M.) 2215–2243 (Lippincott Williams & Wilkins, Philadelphia, 2007).
- Duggal, N. K. & Emerman, M. Evolutionary conflicts between viruses and restriction factors shape immunity. *Nat. Rev. Immunol.* **12**, 687–695 (2012).
- Gifford, R. J. Viral evolution in deep time: lentiviruses and mammals. *Trends Genet.* **28**, 89–100 (2012).
- Kirchhoff, F. Immune evasion and counteraction of restriction factors by HIV-1 and other primate lentiviruses. *Cell Host Microbe* **8**, 55–67 (2010).
- Dawkins, R. & Krebs, J. R. Arms races between and within species. *Proc. R. Soc. Lond. B. Biol. Sci.* **205**, 489–511 (1979).
- Sheehy, A. M., Gaddis, N. C., Choi, J. D. & Malim, M. H. Isolation of a human gene that inhibits HIV-1 infection and is suppressed by the viral Vif protein. *Nature* **418**, 646–650 (2002).
- Laguet, N. et al. SAMHD1 is the dendritic- and myeloid-cell-specific HIV-1 restriction factor counteracted by Vpx. *Nature* **474**, 654–657 (2011).
- Hrecka, K. et al. Vpx relieves inhibition of HIV-1 infection of macrophages mediated by the SAMHD1 protein. *Nature* **474**, 658–661 (2011).
- Neil, S. J., Zang, T. & Bieniasz, P. D. Tetherin inhibits retrovirus release and is antagonized by HIV-1 Vpu. *Nature* **451**, 425–430 (2008).
- Van Damme, N. et al. The interferon-induced protein BST-2 restricts HIV-1 release and is downregulated from the cell surface by the viral Vpu protein. *Cell Host Microbe* **3**, 245–252 (2008).
- Douglas, J. L. et al. The great escape: viral strategies to counter BST-2/tetherin. *PLoS Pathog.* **6**, e1000913 (2010).
- Jia, B. et al. Species-specific activity of SIV Nef and HIV-1 Vpu in overcoming restriction by tetherin/BST2. *PLoS Pathog.* **5**, e1000429 (2009).
- Sauter, D. et al. Tetherin-driven adaptation of Vpu and Nef function and the evolution of pandemic and nonpandemic HIV-1 strains. *Cell Host Microbe* **6**, 409–421 (2009).
- Serra-Moreno, R., Zimmermann, K., Stern, L. J. & Evans, D. T. Tetherin/BST-2 antagonism by Nef depends on a direct physical interaction between Nef and tetherin, and on clathrin-mediated endocytosis. *PLoS Pathog.* **9**, e1003487 (2013).
- Zhang, F. et al. SIV Nef proteins recruit the AP-2 complex to antagonize Tetherin and facilitate virion release. *PLoS Pathog.* **7**, e1002039 (2011).
- Nikovics, K. et al. Counteraction of tetherin antiviral activity by two closely related SIVs differing by the presence of a Vpu gene. *PLoS One* **7**, e35411 (2012).
- Kobayashi, T. et al. Identification of amino acids in the human tetherin transmembrane domain responsible for HIV-1 Vpu interaction and susceptibility. *J. Virol.* **85**, 932–945 (2011).
- Sato, K. et al. Comparative study on the effect of human BST-2/Tetherin on HIV-1 release in cells of various species. *Retrovirology* **6**, 53 (2009).
- Sharp, P. M. & Hahn, B. H. The evolution of HIV-1 and the origin of AIDS. *Philos. Trans. R. Soc. Lond. B Biol. Sci.* **365**, 2487–2494 (2010).
- Wertheim, J. O. & Worobey, M. Dating the age of the SIV lineages that gave rise to HIV-1 and HIV-2. *PLoS Comput. Biol.* **5**, e1000377 (2009).
- Worobey, M. et al. Direct evidence of extensive diversity of HIV-1 in Kinshasa by 1960. *Nature* **455**, 661–664 (2008).
- Gao, F. et al. Origin of HIV-1 in the chimpanzee *Pan troglodytes troglodytes*. *Nature* **397**, 436–441 (1999).
- Keele, B. F. et al. Chimpanzee reservoirs of pandemic and nonpandemic HIV-1. *Science* **313**, 523–526 (2006).
- Hirsch, V. M. et al. An African primate lentivirus (SIVsm) closely related to HIV-2. *Nature* **339**, 389–392 (1989).
- Bailes, E. et al. Hybrid origin of SIV in chimpanzees. *Science* **300**, 1713 (2003).
- Evans, D. T., Serra-Moreno, R., Singh, R. K. & Guatelli, J. C. BST-2/tetherin: a new component of the innate immune response to enveloped viruses. *Trends Microbiol.* **18**, 388–396 (2010).
- Beer, B. E. et al. Characterization of novel simian immunodeficiency viruses from red-capped mangabeys from Nigeria (SIVrcmNG409 and -NG411). *J. Virol.* **75**, 12014–12027 (2001).
- Vinton, C. et al. CD4-like immunological function by CD4⁺ T cells in multiple natural hosts of simian immunodeficiency virus. *J. Virol.* **85**, 8702–8708 (2011).
- Gupta, R. K. et al. Mutation of a single residue renders human tetherin resistant to HIV-1 Vpu-mediated depletion. *PLoS Pathog.* **5**, e1000443 (2009).
- Lim, E. S., Malik, H. S. & Emerman, M. Ancient adaptive evolution of tetherin shaped the functions of Vpu and Nef in human immunodeficiency virus and primate lentiviruses. *J. Virol.* **84**, 7124–7134 (2010).
- Liu, J., Chen, K., Wang, J. H. & Zhang, C. Molecular evolution of the primate antiviral restriction factor tetherin. *PLoS One* **5**, e11904 (2010).
- McNatt, M. W. et al. Species-specific activity of HIV-1 Vpu and positive selection of tetherin transmembrane domain variants. *PLoS Pathog.* **5**, e1000300 (2009).
- Cao, W. et al. Regulation of TLR7/9 responses in plasmacytoid dendritic cells by BST2 and ILT7 receptor interaction. *J. Exp. Med.* **206**, 1603–1614 (2009).
- Zhang, F. et al. Nef proteins from simian immunodeficiency viruses are tetherin antagonists. *Cell Host Microbe* **6**, 54–67 (2009).



36. Galao, R. P. *et al.* Innate sensing of HIV-1 assembly by Tetherin induces NF κ B-dependent proinflammatory responses. *Cell Host Microbe* **12**, 633–644 (2012).
37. Tokarev, A. *et al.* Stimulation of NF- κ B activity by the HIV restriction factor BST2. *J. Virol.* **87**, 2046–2057 (2013).
38. Cocka, L. J. & Bates, P. Identification of alternatively translated Tetherin isoforms with differing antiviral and signaling activities. *PLoS Pathog.* **8**, e1002931 (2012).
39. Fujita, T. *et al.* The candidate proto-oncogene *bcl-3* encodes a transcriptional coactivator that activates through NF- κ B p50 homodimers. *Genes Dev.* **7**, 1354–1363 (1993).
40. Klimkait, T. *et al.* The human immunodeficiency virus type 1-specific protein vpu is required for efficient virus maturation and release. *J. Virol.* **64**, 621–629 (1990).
41. Etienne, L. *et al.* Gene loss and adaptation to hominids underlie the ancient origin of HIV-1. *Cell Host Microbe* **14**, 85–92 (2013).
42. Perelman, P. *et al.* A molecular phylogeny of living primates. *PLoS Genet.* **7**, e1001342 (2011).
43. Goodman, M. *et al.* Toward a phylogenetic classification of Primates based on DNA evidence complemented by fossil evidence. *Mol. Phylogenet. Evol.* **9**, 585–598 (1998).
44. Compton, A. A. & Emerman, M. Convergence and divergence in the evolution of the APOBEC3G-Vif interaction reveal ancient origins of simian immunodeficiency viruses. *PLoS Pathog.* **9**, e1003135 (2013).
45. Chen, Z. *et al.* Natural infection of a homozygous delta24 CCR5 red-capped mangabey with an R2b-tropic simian immunodeficiency virus. *J. Exp. Med.* **188**, 2057–2065 (1998).
46. Riddick, N. E. *et al.* A novel CCR5 mutation common in sooty mangabeys reveals SIVsmm infection of CCR5-null natural hosts and efficient alternative coreceptor use in vivo. *PLoS Pathog.* **6**, e1001064 (2010).
47. National Research Council. Guide for the care and use of laboratory animals (National Academies Press, Washington, D. C., 1996).
48. Tamura, K. *et al.* MEGA5: molecular evolutionary genetics analysis using maximum likelihood, evolutionary distance, and maximum parsimony methods. *Mol. Biol. Evol.* **28**, 2731–2739 (2011).
49. Saitou, N. & Nei, M. The neighbor-joining method: a new method for reconstructing phylogenetic trees. *Mol. Biol. Evol.* **4**, 406–425 (1987).
50. Guindon, S. *et al.* New algorithms and methods to estimate maximum-likelihood phylogenies: assessing the performance of PhyML 3.0. *Syst. Biol.* **59**, 307–321 (2010).
51. Yang, Z. PAML 4: phylogenetic analysis by maximum likelihood. *Mol. Biol. Evol.* **24**, 1586–1591 (2007).
52. Gharib, W. H. & Robinson-Rechavi, M. The branch-site test of positive selection is surprisingly robust but lacks power under synonymous substitution saturation and variation in GC. *Mol. Biol. Evol.* **30**, 1675–1686 (2013).
53. Yang, Z. & dos Reis, M. Statistical properties of the branch-site test of positive selection. *Mol. Biol. Evol.* **28**, 1217–1228 (2011).
54. Zhang, J., Nielsen, R. & Yang, Z. Evaluation of an improved branch-site likelihood method for detecting positive selection at the molecular level. *Mol. Biol. Evol.* **22**, 2472–2479 (2005).
55. Yoshida, I. *et al.* Change of positive selection pressure on HIV-1 envelope gene inferred by early and recent samples. *PLoS One* **6**, e18630 (2011).
56. Carl, S. *et al.* Modulation of different human immunodeficiency virus type 1 Nef functions during progression to AIDS. *J. Virol.* **75**, 3657–3665 (2001).
57. Van Heuverswyn, F. *et al.* Genetic diversity and phylogeographic clustering of SIVcpzPtt in wild chimpanzees in Cameroon. *Virology* **368**, 155–171 (2007).
58. Sato, K. *et al.* Modulation of human immunodeficiency virus type 1 infectivity through incorporation of tetraspanin proteins. *J. Virol.* **82**, 1021–1033 (2008).

Acknowledgments

We would like to thank Drs. Takashi Fujita (Institute for Virus Research, Kyoto University, Japan), Klaus Strebel (National Institute of Allergy and Infectious Diseases, NIH, USA), Frank Kirchhoff (University of Ulm, Germany), and Beatrice Hahn (University of Pennsylvania, USA) for providing p55A2-Luc, pNL43-Udel, pCGCG-IRES-EGFP, and pMB897, respectively. This study was supported in-part by grants from the following: the Aihara Innovative Mathematical Modeling Project, the Japan Society for the Promotion of Science through the “Funding Program for World-Leading Innovative R&D on Science and Technology (FIRST Program),” initiated by the Council for Science and Technology Policy of Japan (to K.S.); Takeda Science Foundation (to K.S.); Sumitomo Foundation Research Grant (to K.S.); Senshin Medical Research Foundation (to K.S.); the intramural research program of NIAID, NIH (to K.M. and V.M.H.); Grants-in-Aid for Scientific Research B24390112 (to Y.Koyanagi) and S22220007 (to Y.Koyanagi) from JSPS; a Grant-in-Aid for Scientific Research on Innovative Areas 24115008 (to Y.Koyanagi) from the Ministry of Education, Culture, Sports, Science and Technology of Japan; and Research on HIV/AIDS (to Y.Koyanagi) from the Ministry of Health, Labor and Welfare of Japan.

Author contributions

T.K., J.S.T., F.R., K.M., K.S., H.T., V.M.H. and Y.Koyanagi wrote the main manuscript text; J.S.T. and F.R. performed molecular phylogenetic analyses and prepared Figure 1; T.K., J.S.T., K.S., Y.Kimura, N.M., R.Y., Y.N. and E.Y. performed the experiments and prepared Figures 2–4; K.M. and V.M.H. contributed to the samples of RCM genomic DNA; K.S. conceived and designed the experiments. All authors reviewed the manuscript.

Additional information

Supplementary information accompanies this paper at <http://www.nature.com/scientificreports>

Competing financial interests: The authors declare no competing financial interests.

How to cite this article: Kobayashi, T. *et al.* Characterization of red-capped mangabey tetherin: implication for the co-evolution of primates and their lentiviruses. *Sci. Rep.* **4**, 5529; DOI:10.1038/srep05529 (2014).



This work is licensed under a Creative Commons Attribution-NonCommercial-ShareAlike 4.0 International License. The images or other third party material in this article are included in the article's Creative Commons license, unless indicated otherwise in the credit line; if the material is not included under the Creative Commons license, users will need to obtain permission from the license holder in order to reproduce the material. To view a copy of this license, visit <http://creativecommons.org/licenses/by-nc-sa/4.0/>